

Numerical Evaluation of Press Forming Parameters and Mould Geometry in Wood Plastic Composite(WPC) Products

Sami Matthews^{1,a*}, Panu Tanninen^{2,b}, Amir Toghiani^{1,c}, Ville Leminen^{2,d}
and Juha Varis^{1,e}

¹Research group of Production Engineering, LUT University, Finland

²Research group of Packaging Technology, LUT University, Finland

^asami.matthews@lut.fi, ^bpanu.tanninen@lut.fi, ^camir.toghiani@lut.fi, ^dville.leminen@lut.fi,
^ejuha.varis@lut.fi

Keywords: press-forming, mould design

Abstract. The purpose of this paper is to investigate factors associated with press-forming of Wood Plastic Composite (WPC) products. The WPC material is a novel, feasible, and economic way to use recycled thermoplastics. Due to the complexity of the fiber-polymer interaction, numerical simulation and thus prediction of WPC behavior in forming have been challenging. Up to now, press moulds have had to be empirically validated. In this paper, we explore the possibility of predicting material behavior using Autodesk Moldflow.

Introduction

Wood-plastic composite (WPC) is a broad category of composite materials containing plant fibers on a thermoset or thermoplastic matrix. The properties of WPCs are determined primarily by the fiber and polymer components. Recent years have seen an increase in the use of WPC products due to its many advantages, including its improved dimensional stability and higher resistance to decay, compared with plain wood products [1]. It also has the advantages of low abrasiveness, high stiffness, wide availability, and biodegradability [2]. WPC material is used in various indoor and outdoor applications, such as decking, railing, fencing, roofing, siding, and landscaping timbers [3]. WPC is a good example of a modern material that has the potential to become even more popular through the use of recycled source materials that will bring cost savings, as well as potential environmental benefits. [4].

Injection moulding of composite materials can be challenging due to the fact that fibers are significantly larger than polymer molecules and do not melt. This can result in a blockage in the injection mold gate or runner, making injection molding difficult. As a result, WPC products are usually press-formed in compression molding. Compression molding differs from injection molding in that a charge or sheet of semi-molten material is placed into an open cavity, which is then mechanically compressed to fill and pack the cavity. A primary advantage of these processes is the ability to produce dimensionally stable, relatively stress-free parts with significantly lower clamping force. It is known that during the compression strain rate[5] and WPCs as polymer-based materials are highly related to the temperature of the material and also the matrix polymer group, and that the performance of high-density polyethylene (HDPE) and HDPE-based composites is greatly dependent on the temperature and processing time of manufacturing [6][7].

Simulation of composite material compression molding is a computationally very demanding and time-consuming task that often requires the use of supercomputer clusters. The Autodesk Moldflow® software is relatively easy and convenient way to simulate aspects of this dynamic process in comparison to full-fledged explicit FEA solvers like Abaqus. An example application of Moldflow is the simulation of the compression press-forming of recycled ABS composites [8].

The purpose of this paper is to investigate the effects of warpage and shrinkage caused by polymer matrix of composite material by measuring the physical samples and comparing them to a numerical model.

Methods

This chapter provides the tested key parameters affecting compression forming.

Used wood plastic composite material. Preformed extruded composite material sheets with the dimensions of 200 mm x 200 mm x 3 mm are cut and reheated to set temperatures in an electric oven.

Used WPC material consists of 50% recycled HDPE, 44% Wood flour(MESH 20), 3% MAPE, 3% Lubricant. Following experimental data in Table 1 was obtained from standard set of material tests [9-11].

Table 1. Measured experimental values based on ASTM D638-10, ASTM D790-17 and ASTM E1269-11.

Modulus of elasticity	3550	MPa
Shear modulus	1431	MPa
Poissons ratio	0.39	
Tensile strength	8.2	MPa
Melt density	983	g/cm ³
Specific heat (150 C)	2550	J/kgC

Physical setup. The maximum press punching force is set to 4 kN. A circular plate with a target diameter of 150 mm and a wall thickness of 3 mm is used for physical and numerical tests. Its uniform shape facilitates evaluation measurements, simplifies the assessment of the factors involved, and provides reliable baseline results that can be used in studies of more complex and non-symmetrical shapes. The forming tools consists of a male punch and female die (Figure 1).

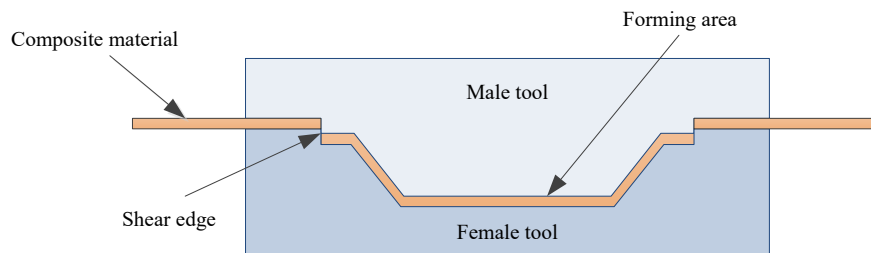


Fig. 1. The highlighted shear edges cut and trim the product, while the forming area forms the product geometry.

For non-destructive wall thickness analysis resulting geometry is 3D surface scanned with Hexagon Metrology Romer HP-L-20.8 laser scanner attached RA-7520 SE measurement arm. The resulting STL surface model is colorized and rendered in Blender 3.0 -software.

Numerical simulation setup. For numerical evaluation Autodesk Moldflow® Insight 2021(AMI) software is used together with Moldflow Synergy 2021- graphical user interface. Moldflow is a finite volume solver commonly used to simulate the flow, cooling, and warpage of injection or compression molding processes. As a result, it helps solve the typical challenges and delays of injection and compression molding, as well as optimize the part and mold.

Numerical simulation was done using Thermoplastics Compression Molding-simulation model with Fill + Pack + Warp analysis sequence.

Based on data collected from neat HDPE material and the experimental data, a new material dataset is created. Fiber orientation characteristics is simulated using Mudflow Rotational Diffusion model based on Folgar-Tucker orientation equation.

The object is meshed with volumetric 3D tetrahedral elements of 2 mm length for a total count of 399876 elements. The simulation series were set according to the table 2.

Table 2. The tested press forming parameters in physical and AMI-simulation time.

Series name	a	ct1	ct2	mt1	mt2	ss1	ss2
Press compression time (s)	5	1	10	5	5	5	5
Melt temperature (C)	150	150	150	130	170	150	150
Stroke speed (mm/s)	20	20	20	20	20	50	100

A-series is the basic set of parameters used for comparisons with the other variables. Ct-series represents variable compression time, and it is set based on a range that is feasible for rapid mass production. Mt-series variates temperature of melting in a way that the wood fibers are not permanently damaged during the heating process. Ss-series stands for stroke speed, which offers a range of typical hydraulic press speeds.

Results

This chapter presents and compares the results of physical and numerical forming tests.

Shrinkage and diameter change. Figures 2 and 3 illustrate the warpage and shrinkage in one example specimen.

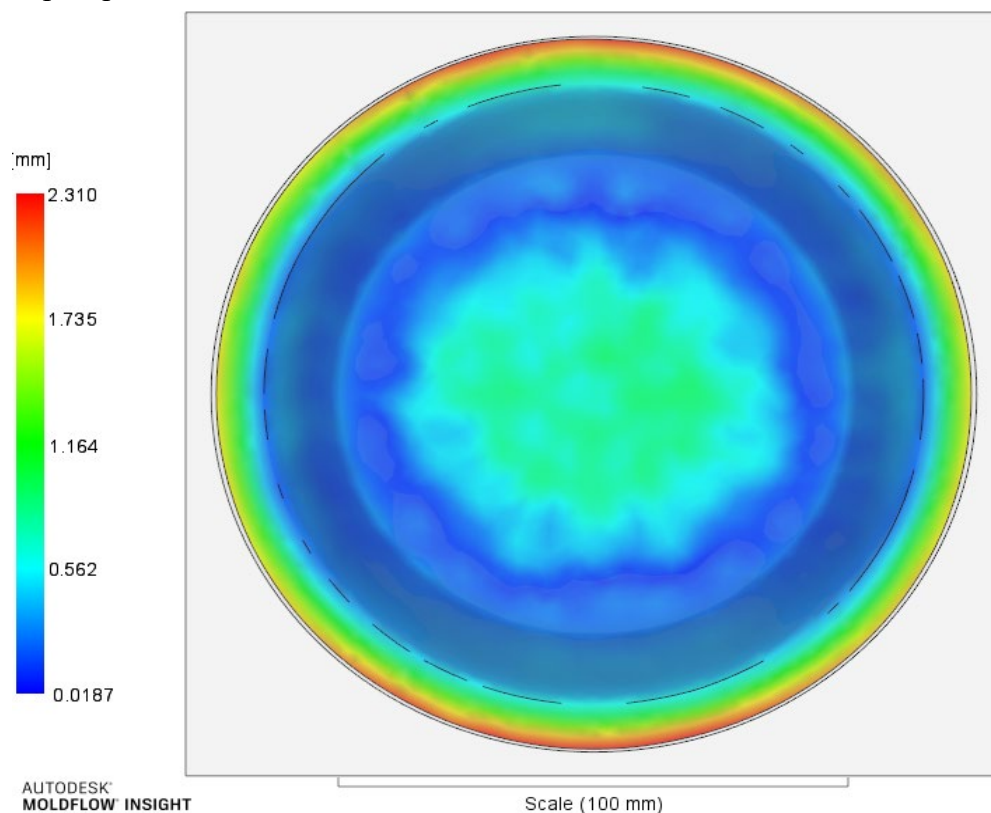


Fig 2. The figure illustrates the warpage and shrinkage of the composite material after cooling. An indication of anisotropic fiber orientation is evident in the displacement and elongation in vertical direction of the figure.

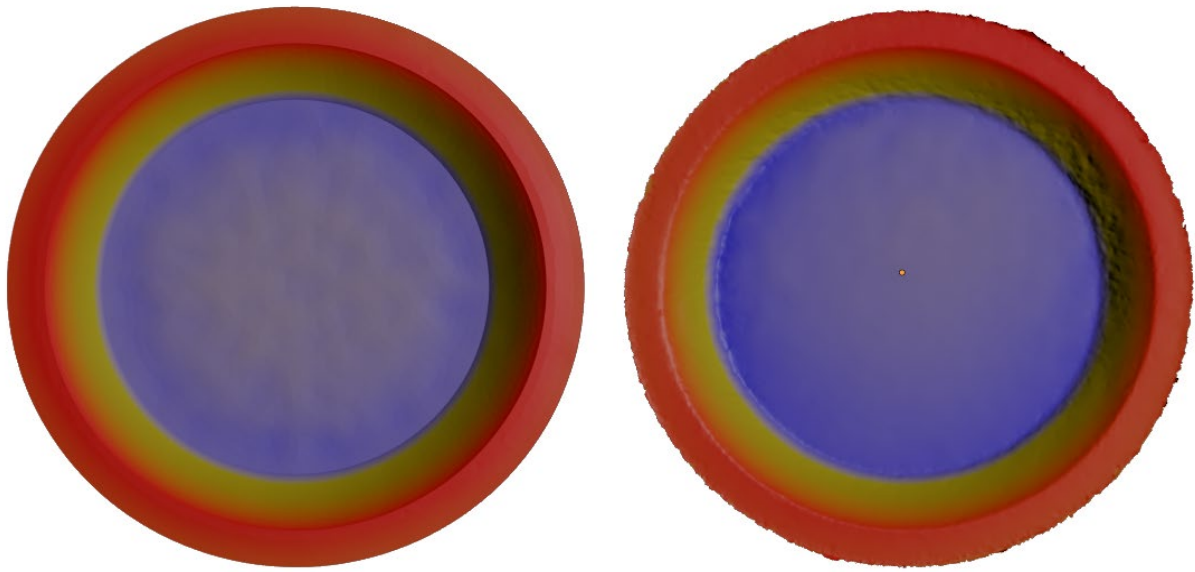


Fig. 3. Figure presents comparison of plate depth. Numerical model generated in Moldflow is located on left and physical surface scanned model is located on right. Blue color denotes deeper and red color shallower area in the palette.

Table 3 provides the results of diameter measurements and compares them to the simulated results. The Pearson correlation coefficient is then used to correlate the resulting variables in table 4.

Table 3. The results to overall diameter. (FB denotes fiber direction, CD counter direction and STDEV denotes to standard deviation calculated from all specimen.

Series	FD actual (mm)	STDE V	CD actual (mm)	STDE V	FD simulated (mm)	CD simulated	Diff. FD (%)	Diff. CD (%)
a	148,9	0,62	146,9	0,51	148,5	147,3	-0,269	0,272
ct1	148,9	0,57	146,9	0,51	148,5	147,3	-0,269	0,272
ct2	148,6	0,35	147,3	0,21	148,2	147,1	-0,270	-0,136
mt1	148,9	0,51	147,5	0,67	N/A	N/A	N/A	N/A
mt2	148,3	0,2	146,3	0,17	149,0	147,4	0,470	0,746
ss1	148,3	0,33	146,5	0,23	148,5	147,3	0,135	0,543
ss2	148,9	0,61	146,9	0,51	148,5	147,3	-0,269	0,272

Table 4. Pearson correlation coefficient between variables. Blue background color denotes positive correlation while red background color denotes negative correlation.

	FD		CD		FD simulated	CD		Diff. FD	Diff. CD
	actual	STDEV	actual	STDEV		simulated	Diff. FD		
Compression time	-0.288	-0.387	0.307	-0.457	-0.355	-0.539	-0.027	-0.362	
Temperature	-0.607	-0.549	-0.832	-0.742	0.864	0.764	0.843	0.829	
Stroke Speed	0.107	0.288	-0.158	0.100	0.032	0.227	-0.045	0.175	

Thickness variation. Figures 3 and 4 demonstrate the direction warpage and potential effects on thickness variation.

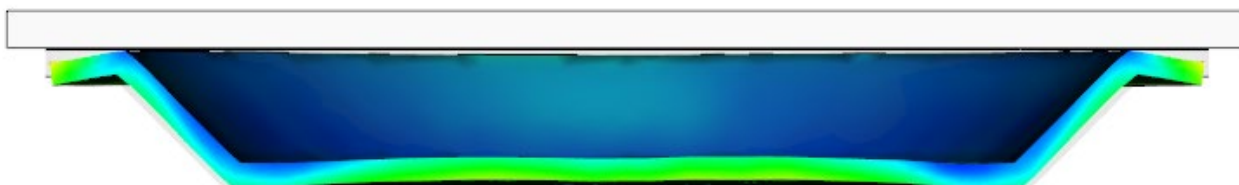


Fig. 4. Cut-section of the plate is illustrated. The direction of warp after cooling can be observed.



Fig. 5. Cut-section of surface scanned plate.

The dimensions of the observed wall thickness are presented in Table 5. To correlate the variables in table 6, the Pearson correlation coefficient is used.

Table 5. The results of the wall thickness. STDEV denotes to standard deviation calculated from all specimen.

Series	Edge measured (mm)	STDEV	Center measured (mm)	STDEV	Edge simulated (mm)	Center simulated (mm)	Diff. Edge(%)	Diff. Center(%)
a	2,59	0,16	2,81	0,22	2,47	2,41	-4,9	-16,6
ct1	2,53	0,09	2,95	0,32	2,45	2,42	-3,3	-21,9
ct2	2,53	0,17	2,72	0,14	2,81	2,69	10,0	-1,1
mt1	2,61	0,19	2,79	0,27	N/A	N/A	N/A	N/A
mt2	2,51	0,21	2,98	0,35	2,75	2,90	8,7	-2,8
ss1	2,61	0,39	2,79	0,35	2,91	3,11	N/A	N/A
ss2	3,02	0,34	3,18	0,45	2,55	2,39	-18,4	-33,1

Table 6. Pearson correlation coefficient between variables. Blue background color denotes positive correlation while red background color denotes negative correlation.

	Edge thickness	STD EV	Center thickness	STDE V	Edge simulated	Center simulated	Diff. FD	Diff. CD
Compression time	-0.035	0.162	-0.438	-0.558	0.542	0.258	0.366	0.399
Temperature	-0.163	0.055	0.346	0.229	-0.094	0.220	0.043	0.019
Stroke speed	0.948	0.751	0.702	0.733	-0.099	-0.158	-0.669	-0.466

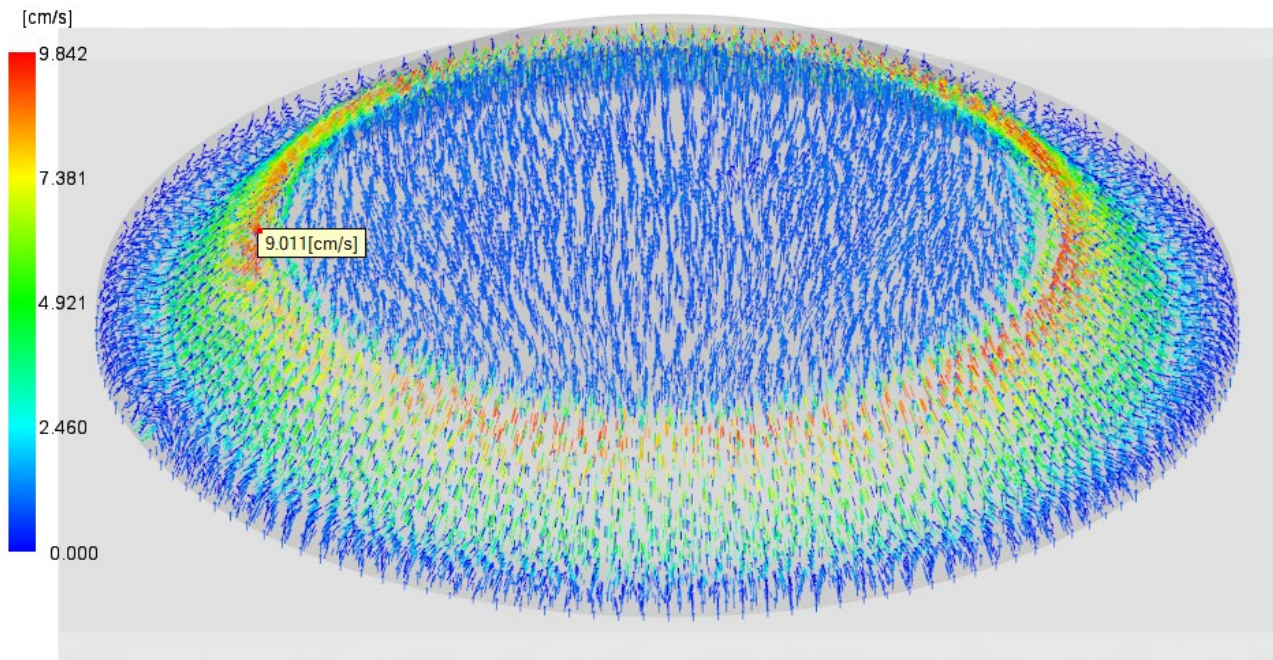


Fig. 6. Speed vectors of material flow during compression molding. Maximum speeds were observed near the edge of plate center face.

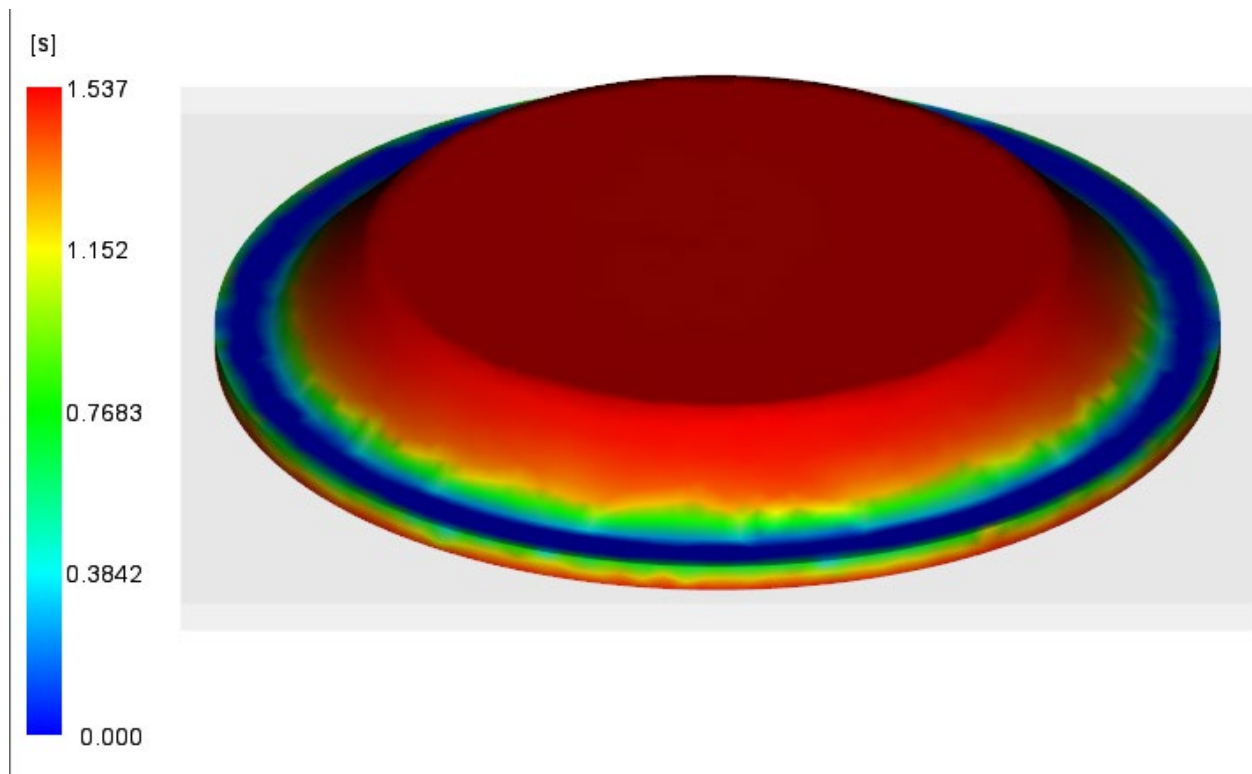


Fig. 7. Compression fill time of the plate at stroke speed of 10 mm/s.

Figures 6 and 7 illustrate material flow rate and duration to the flat bottom of the plate specimen.

Discussion

Press compression time has relatively low correlations (0.25-0.540) to the diameter and thickness. This is contrary to analogous paperboard laminate material where compression time has strong correlation to the overall diameter [12-13].

Melt temperature has a strong positive correlation to the simulated diameter results while there is similar but negative correlation to the physical measurements. This correlation is mostly not evident in thickness measurements. At 130 C, the numerical model failed, because at least one element was deemed to be prematurely solid, so the software skipped this step and began analyzing the packing automatically. As a result, the software simulation cannot be used in close proximity to the melting temperature of the material.

Stroke speed has a strong influence in physical measurement on edge thickness and center thickness, however the correlation is not significant in case of numerical simulation. This behavior is likely the result of trapped air under compression, even though both the physical and simulated models had a circular vent hole at the center.

The Moldflow compression analysis took an average of 19 minutes on Intel i7 9700K octa-core processor, which made it a suitable tool for rapid investigation of the distribution of material and for gaining better understanding of what is happening in depth.

One limitation of this study was that the press force was set as constant. It has been observed in analogous paperboard materials that the press-forming force resulting from a variable force curve has a significant impact on quality[14]. The force curve can be incorporated into Moldflow and the impact could be studied in the future.

The simulated results did not have any numerical variation while the physical sheet thickness varied locally ± 0.1 mm and this is one missing factor in this study. Probably as a consequence, the observed difference in thickness was greater than that observed in the diameter analysis.

In this investigation evaluation of effect of fiber arrangement and disposition was still limited, for example the Moldflow allows to use much more sophisticated models such as Anisotropic Rotary Diffusion(ARD) for relatively long fibers (more than 1 mm) as presented by Phelps and Tucker[15], this feature could be investigated in future.

Conclusions

This paper investigated the effects of warpage and shrinkage caused by polymer matrix of composite material by measuring the physical samples and comparing them to a numerical model.

In experimental press-forming process, combining the physical tests with numerical simulation model in Autodesk Moldflow enables better prediction and comprehension of the composite material behavior. The results demonstrate that:

- Moldflow can estimate the success in compression moulding of fiber composite materials as long as the material temperature parameter is selected well above the melting point of the polymer matrix. The program is not usable in simulation of press-forming at semi-molten temperatures.
- Material solidification time and temporal diameter warpage correspond to the results of physical testing.
- Prediction of fiber orientation and even distribution is only indicative at best in Moldflow with the default fiber orientation model.

Acknowledgements

This article was funded by European Council LIFE15 IPE FI 004 project Circwaste.

References

- [1] R. Steward, Wood fiber composites: Fierce competition drives advances in equipment, materials and processes, *Plast. Eng.* 63 (2007) 21-28.
- [2] D.B. Dittenber, H.V.S. Gangarao, Critical review of recent publications on use of natural composites in infrastructure, *Compos. Part Appl. Sci. Manuf.* 43 (2012) 1419–1429.
- [3] A. Ashori, Effects of nanoparticles on the mechanical properties of rice straw/polypropylene composites, *J. Compos. Mater.* 47 (2013) 149-154.
- [4] A. Ashori, A. Nourbakhsh, Characteristics of wood-fiber plastic composites made of recycled materials, *Waste Manag.* 29 (2009) 1291-1295.
- [5] A. Toghyani, A. Mohsen, Effect of strain rate and temperature on press forming of extruded WPC profiles, *Composite Structures* 180 (2017) 845-852.
- [6] Y. Bai, T. Keller, T. Vallée, Modeling of stiffness of FRP composites under elevated and high temperatures, *Compos Sci Technol*, 68 (15–16) (2008) 3099-3106.
- [7] R. Huang, B.J. Kim, S. Lee, Y. Zhang, Q. Wu, Co-extruded wood-plastic composites with talc-filled shells: morphology, mechanical, and thermal expansion performance, *Bioresources*, 8 (2) (2013) 2283-2299.
- [8] C. Vardaan, T. Kärki, J. Varis, Optimization of Compression Molding Process Parameters for NFPC Manufacturing Using Taguchi Design of Experiment and Moldflow Analysis, *Processes* 9 (2021) 1853–1863.
- [9] ASTM D638-10 Standard Test Method for Tensile Properties of Plastics, ASTM International (2010).
- [10] ASTM D790-17 Standard Test Methods for Flexural Properties of Unreinforced and Reinforced Plastics and Electrical Insulating Materials, ASTM International (2017).
- [11] ASTM E1269-11 Standard Test Method for Determining Specific Heat Capacity by Differential Scanning Calorimetry, ASTM International (2018).
- [12] P. Tanninen, V. Leminen, S. Matthews, M. Kainusalmi, J. Varis, Process cycle optimization in press forming of paperboard, *Packaging Technology and Science* 31 (2018) 369–376.
- [13] V. Leminen, S. Matthews, P. Tanninen, J. Varis, Effect of creasing tool dimensions on the quality of press-formed paperboard trays, *Procedia Manuf.* 25 (2018) 397–403.
- [14] P. Tanninen, V. Leminen, A. Pesonen, S. Matthews, J. Varis, Surface fracture prevention in paperboard press forming with advanced force control, *Procedia Manuf.* 47 (2020) 80–84.
- [15] J. Phelps, C. L. Tucker, An Anisotropic Rotary Diffusion Model for Fiber Orientation in Short- and Long-Fiber Thermoplastics. *J. Non-Newtonian F. Mech.* 156 (2009) 165–176.